Supplementary Material

Sceptic priors and climate consensus

Grant McDermott

Contents

Sensitivity analysis

As noted in the main text, I consider a number of alternative specifications to test the sensitivity of my findings. The following section provides additional context and technical information for these different sensitivity runs.

Note: Figs. SM1 – SM8 are directly comparable to Fig. 1 in the main text and the same general notes apply (dashed lines denote TCR priors, solid lines denote TCR posteriors, etc.) In some cases, the x-axis has been truncated to preserve this direct comparability, though the posterior distributions extend beyond the -1 °C to 3 °C range. The caption of each figure references against the key listed in Table 4 of the main text.

Alternative GMST series

HadCRUT4 is known to suffer from potential coverage biases due to incomplete placement of in situ thermometers. I therefore rerun the analysis with two alternate reconstructions of GMST. Cowtan and Way [2014], hereafter CW14, correct for the gaps in the HadCRUT4 dataset by using an interpolation algorithm based on the "kriging" method.[1] Similarly, the NASA Goddard Institute for Space Studies uses an extrapolation algorithm to overcome coverage bias in GISTEMP, its own GMST reconstruction. Running the Bayesian regression model on these alternative series yields moderately higher TCR values compared to HadCRUT4. Under a noninformative prior, the posterior TCR means (and 95% Bayesian credible intervals) are 1.6 °C (1.4–1.9 °C) for CW14 and 1.8 °C (1.5–2.0 °C) for GISTEMP. Given that the explicit goal of this paper is to evaluate policy options from the perspective of climate sceptics, I continue using the results from the HadCRUT4 series as a default. Yet, it should be noted that this is a conservative choice that may, at least marginally, understate the true level of warming.
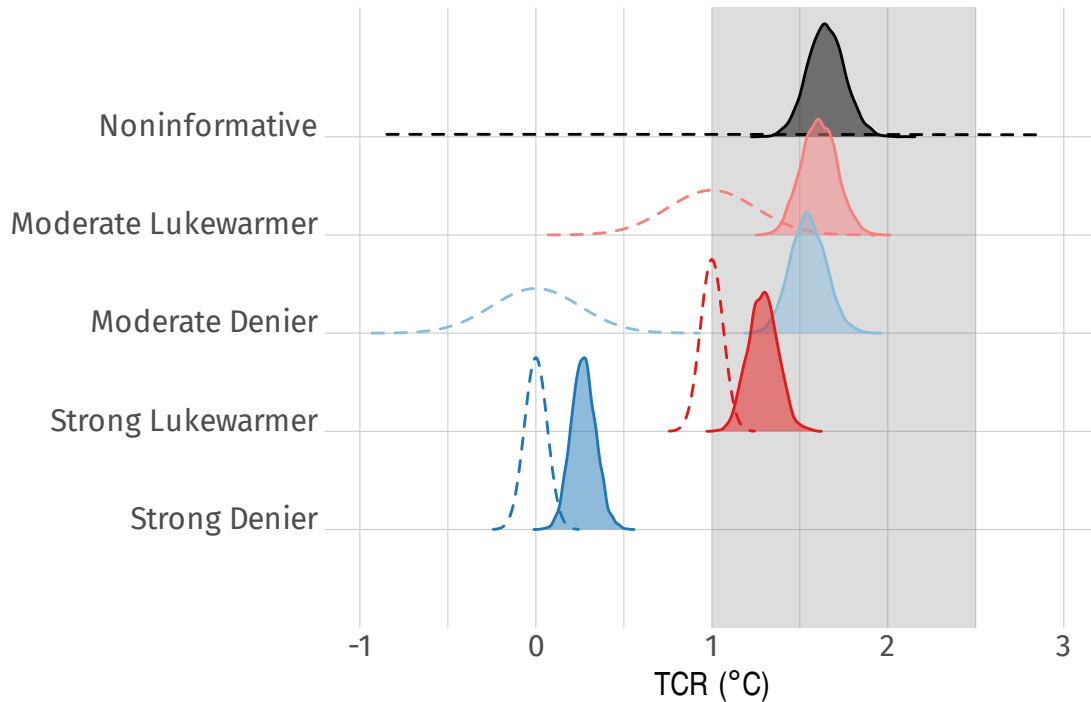

Figure SM1: TCR densities: "CW14" sensitivity run.

---

[1]HadCRUT5 [Morice et al., 2020], released during the late revision stages of this manuscript, adopts a similar interpolation strategy to CW14. We would consequently expect this updated version of the HadCRUT temperature record to yield similar posterior results as CW14.
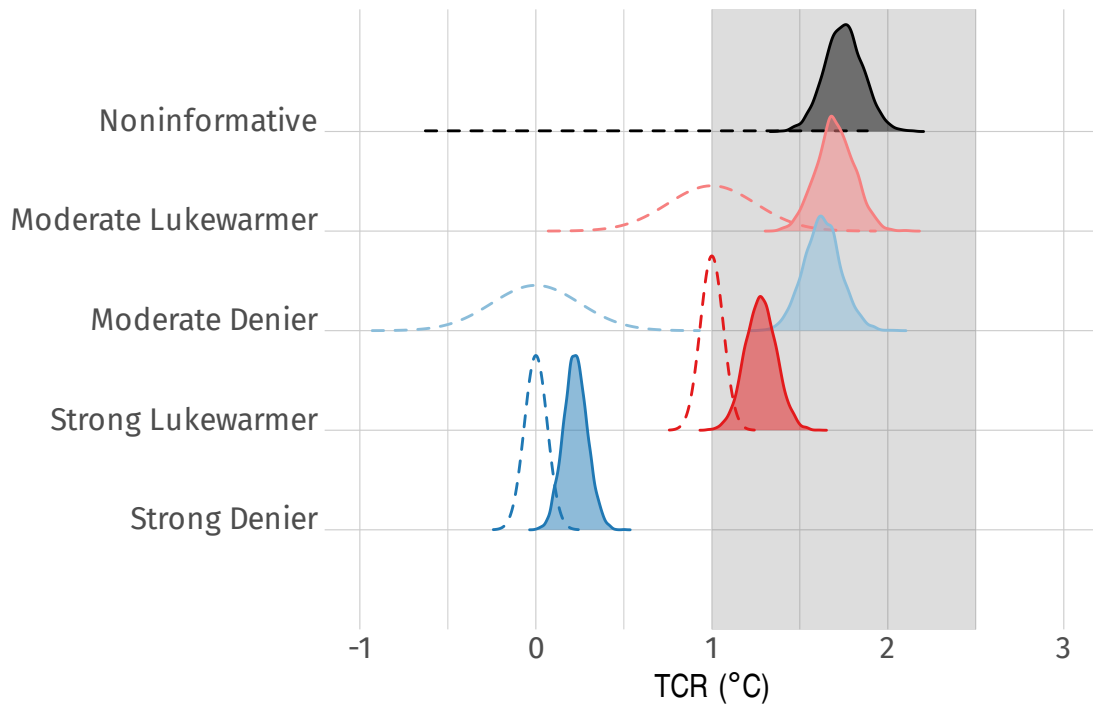
Figure SM2: TCR densities: "GISTEMP" sensitivity run.

Measurement error in GMST data

All three GMST reconstructions used in this study provide estimates of measurement error. The Bayesian framework is ideally suited to incorporate such knowledge, since the nested model structure allows us to fully specify measurement error on the dependent variable within the regression model itself. Doing so under the noninformative prior yields TCR estimates of 1.6 °C (1.4–1.8 °C), which are effectively identical to the comparable result in the main text. This is unsurprising once we recall that measurement error on the dependent variable is absorbed by the disturbance term of the regression model.[2] Since the Bayesian regression framework is primarily concerned with total model uncertainty, specifying the relative contribution of such measurement error to the overall disturbance doesn't meaningfully alter the analysis — though it may be useful for incorporating known sources of heteroscedasticity.[3] The primary regression results already have GMST measurement error "baked in" to the estimation, regardless of whether we define it explicitly or not.
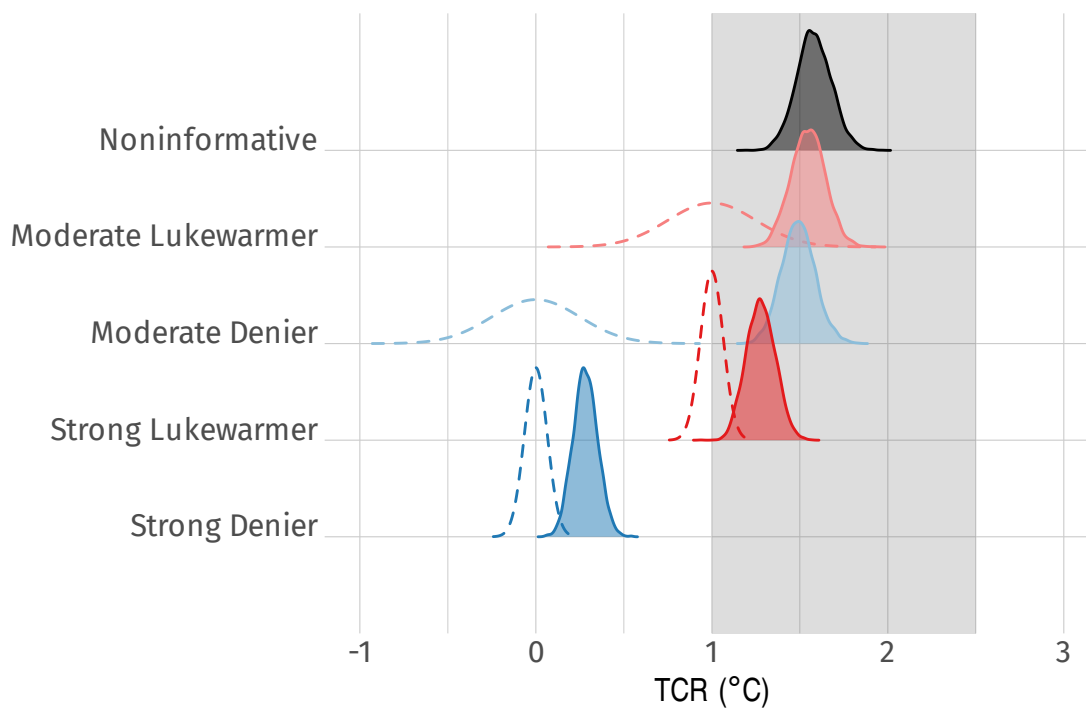

Figure SM3: TCR densities: "HadCRUT ME" sensitivity run.

---

[2]For example, see [Greene, 2007, p. 326]. To illustrate with a simple univariate case: The regression model can be written as $y_t \sim \mathcal{N}(\beta X_t, \sigma^2 + \omega_t^2)$, where $\sigma^2 = \mathrm{Var}(\epsilon)$ is the variance of the error term and $\omega_t^2 = \mathrm{Var}(\nu_t)$ is the variance of the measurement error on y_t. Together, ϵ and ν_t make up the overall disturbance of the regression.

[3]See Lewis and Linzer [2005] for a related discussion in a frequentist setting.

Measurement error in forcings data

While measurement error in the dependent variable is already (i.e. implicitly) encapsulated by my Bayesian regression model, the same cannot be said of any explanatory variables. In particular, uncertainty about the radiative forcing data would need to be accounted for explicitly in the modeling procedure. Fortunately, the Bayesian framework offers a natural way to incorporate this type of uncertainty. I conduct a Monte Carlo simulation using the 1,000-member ensemble of forcing estimates from Dessler and Forster [2018]; hereafter DF18. Specifically, I run my Bayesian regression model on each member of the DF18 ensemble separately — 1,000 different regressions with each taking their corresponding forcings as the true state of the world — before aggregating the posterior results into a single meta-distribution at the end.[4] The resulting posterior distributions are wider, as expected due to the additional uncertainty. But the noninformative TCR mean and 95% credible interval of 1.4 °C (0.9–2.6 °C) are still well situated within the IPCC "likely" range.
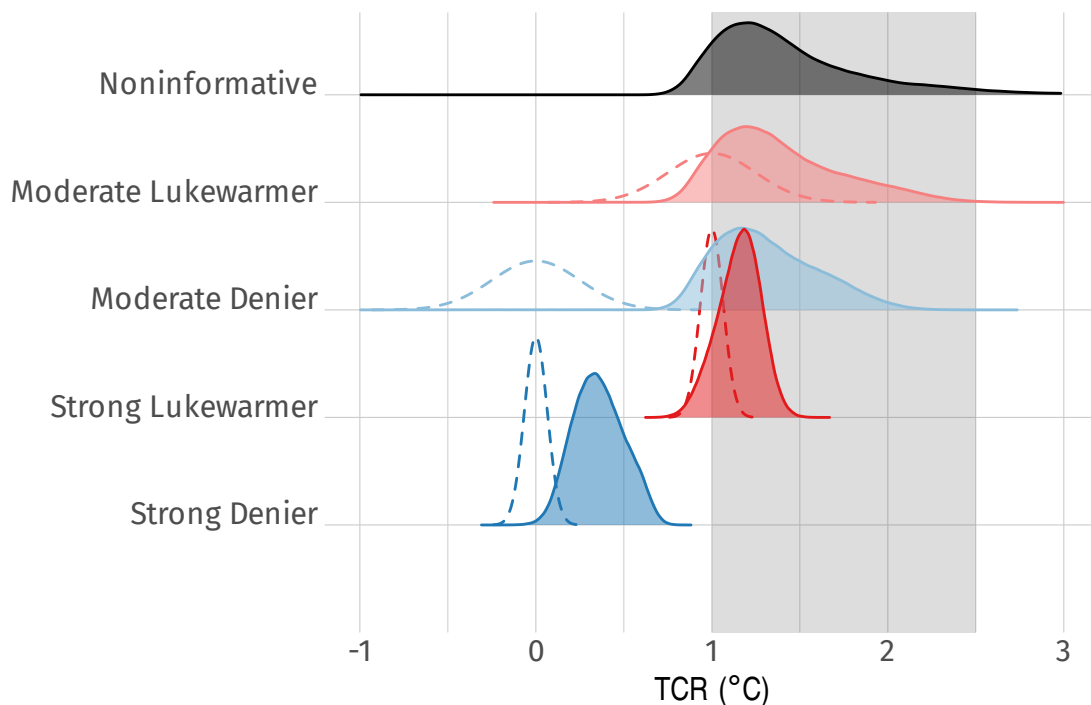

Figure SM4: TCR densities: "DF18" sensitivity run.

---

[4]This probabilistic approach is the standard Bayesian solution to dealing with measurement error in explanatory variables. In contrast, deriving consistent regression estimators when there is measurement error in explanatory variables can be a much more complicated affair in frequentist settings [Greene, 2007].

Adjusted forcing efficacies

The regression models in the main text implicitly assume that the different physical drivers making up total radiative forcing have the same per-unit effect on GMST. Forcing agents that yield a similar radiative imbalance in Wm^{-2} are expected to result in similar feedbacks and responses in GMST. However, recent research has suggested that the warming efficacy of different forcing agents can, in fact, vary with factors like geography. Aerosol emissions, for example, are primarily concentrated in the mid-to-high latitudes of the Northern Hemisphere. The disproportionately large land mass in this region causes aerosol forcing to exhibit stronger feedback effects and an accelerated temperature response than if it were uniformly distributed across the globe Shindell [2014].

The implications of such forcing inhomogeneity on climate sensitivity estimates are more fully explored by Marvel et al. [2016], hereafter MEA16. I adapt their results to construct an adjusted series of total radiative forcing, where each forcing agent is pre-multiplied by an appropriate efficacy coefficient (see Supplementary Material). Specifically, I consider two approaches. The first takes MEA16's mean efficacy estimates as given and ignores all modeling uncertainty in their results. The second explicitly accounts for modeling uncertainty in much the same way that was used to account for explanatory variable measurement error above; i.e. I conduct a Monte Carlo exercise that repeatedly samples from the t distributions underlying each forcing efficacy estimate and then combines the posterior results from many regressions into a single meta-distribution at the end. Consistent with MEA16, both approaches lead to a pronounced increase in the posterior TCR mean, with the Monte Carlo sampling approach further yielding a much wider credible interval. However, MEA16 note that data artefacts — e.g. small changes experienced by some forcing agents over their study period — automatically induce large uncertainties in the associated efficacy estimates. Combined with the fact that MEA16 obtain their results from a single climate model rather than a multi-model ensemble, this means that the unusually wide credible intervals of the latter Monte Carlo approach should be regarded with caution.

Table SM1: TCR efficacies used in "MEA" I and II sensitivity runs

Forcing agent	Mean	95% C.I.
Aerosols	1.55	(1.05, 2.05)
GHGs	1.17	(1.07, 1.28)
Land use	3.82	(-2.16, 9.80)
Ozone	0.66	(0.34, 0.98)
Solar	1.68	(-1.27, 4.63)
Volcanic	0.61	(0.33, 0.89)

Notes: Adapted from Table S1 of Marvel et al. [2016]. Confidence intervals on the sample means are constructed from a t distribution with 4 degrees of freedom.
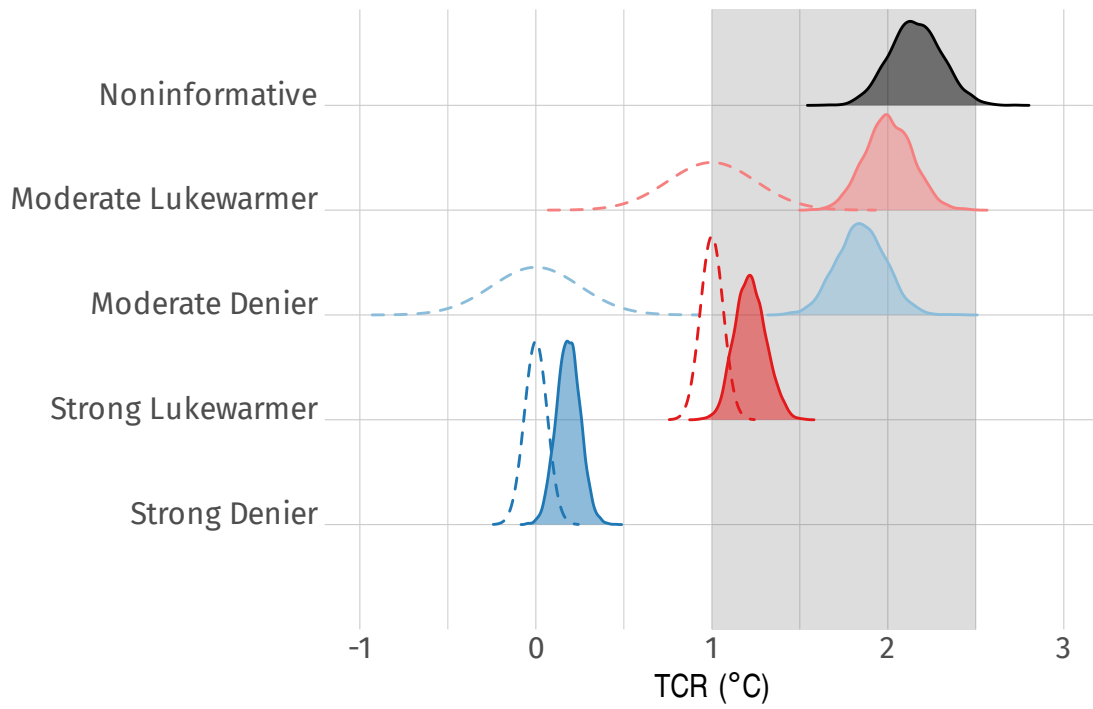
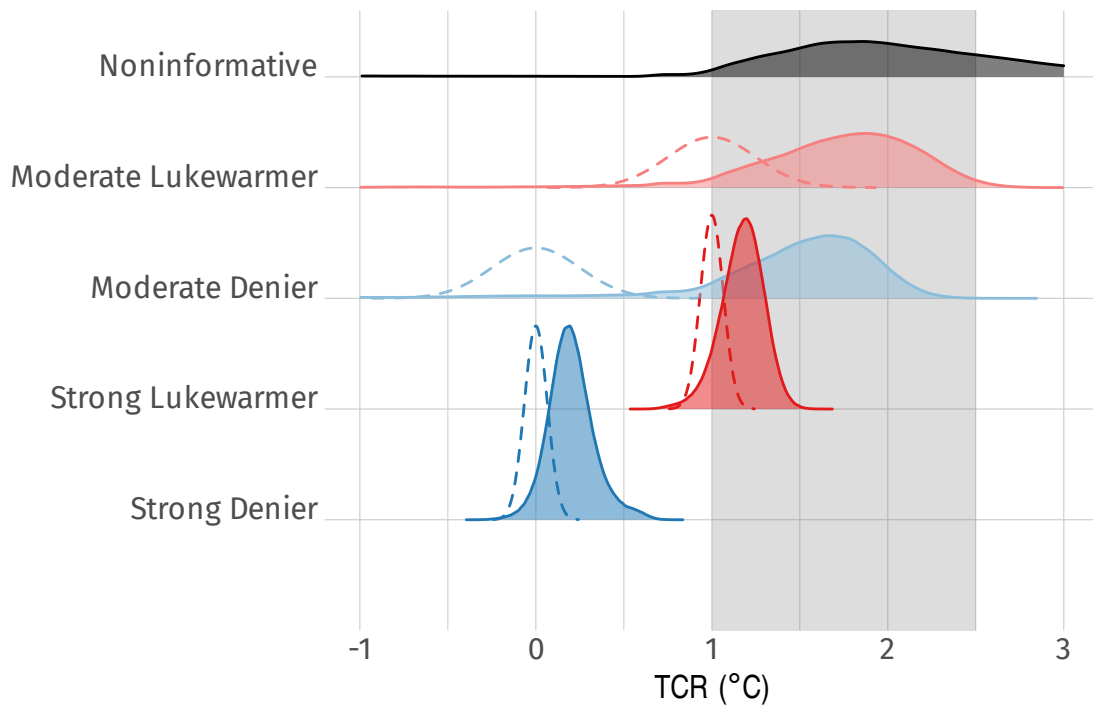Figure SM5: TCR densities: "MEA I" sensitivity run.

Figure SM6: TCR densities: "MEA II" sensitivity run.

Separate anthropogenic forcings (CO$_2$) from other forcings

As final sensitivity test, I relax the constraint that all sources of radiative forcing have to be included in the regression model under the same composite RF term. As described in the main text, this decision was motivated by the fact that the forcing agents in my dataset are all defined in Wm^{-2}. Separating out individual forcings and then placing different priors on them will likely cause the model to become physically inconsistent.[5] Such admonishments notwithstanding, I implement two version of this unphysical model. The first separates out anthropogenic forcings (e.g. GHGs) from natural forcings (e.g. solar radiation). The second separates out CO$_2$ forcing from all other sources. In each case, the subjective sceptic priors are placed only on the isolated anthropogenic component. All other variables take noninformative priors. Both sets of regressions yield very similar results to the main, physically-correct specification. If anything, isolating CO$_2$ on its own yields a higher posterior TCR for certain prior types. However, this latter implementation should be treated with caution for reasons previously described.
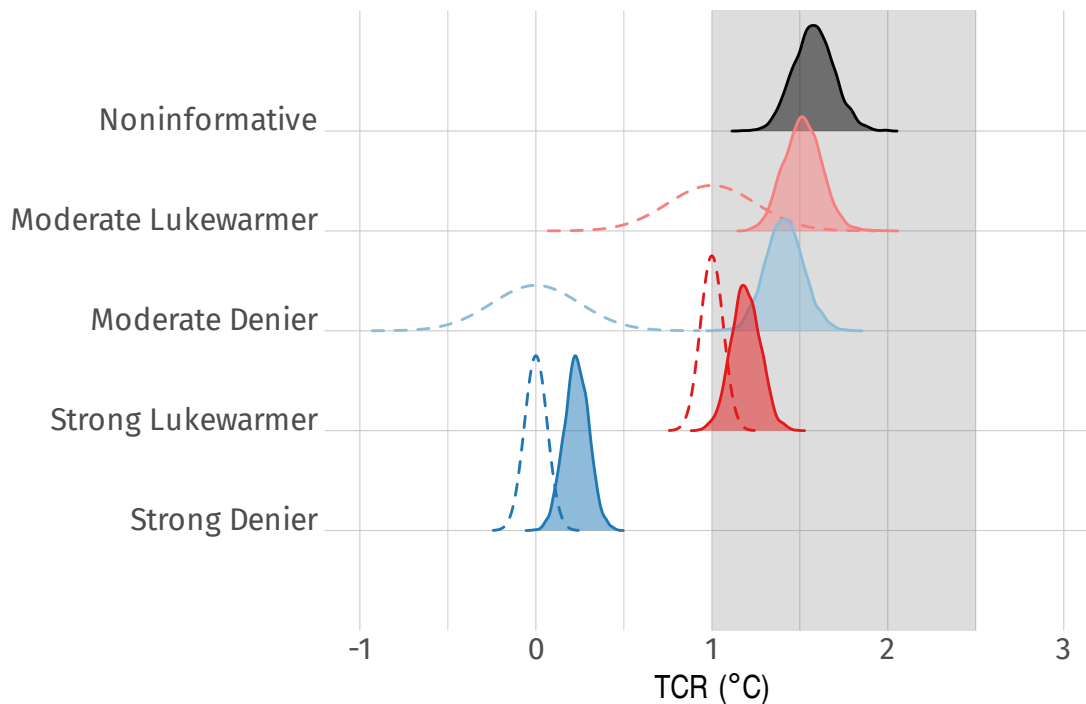

Figure SM7: TCR densities: "Anthro" sensitivity run.

---

[5]For the anthropogenic forcings, the use of a composite term also avoids introducing severe multicollinearity into the econometric estimation.

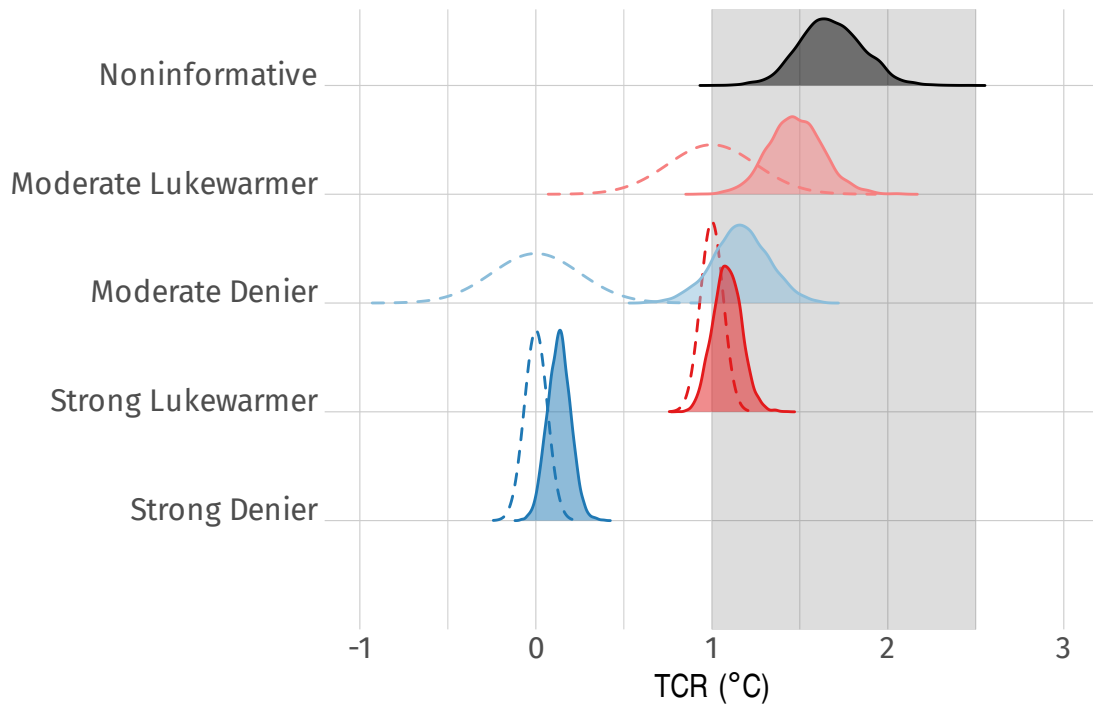Figure SM8: TCR densities: "CO2" sensitivity run.

Future temperatures

Table SM2: Covariate vectors for 2100 predictions

	RCP 2.6	RCP 4.5	RCP 6.0	RCP 8.5
RF_{2100}	2.626	4.281	5.522	8.340
CO$_2$ component	85%	83%	86%	78%
Solar component	7%	4%	3%	2%
$\overline{VOLC}$	0.017	0.017	0.017	0.017
$\overline{SOI}$	-0.079	-0.079	-0.079	-0.079
$\overline{AMO}$	-0.002	-0.002	-0.002	-0.002

Notes: Covariates are used to predict the global mean surface temperature anomaly in the year 2100. The Representative Concentration Pathways (RCPs) are a family of forcing scenarios developed for the IPCC Van Vuuren et al. [2011]. Each RCP has a core component of atmospheric CO$_2$ concentrations, measured in parts per million volume (ppmv). With regard to the covariates in the regression model, total radiative forcing (RF) and volcanic aerosols ($VOLC$) are measured in Wm^{-2}. The Southern Oscillation Index (SOI) and Atlantic Multidecadal Oscilliation (AMO) are measured as scaled indices. Future values for RF are taken from the RCP database. For the rest, historical mean values are used.
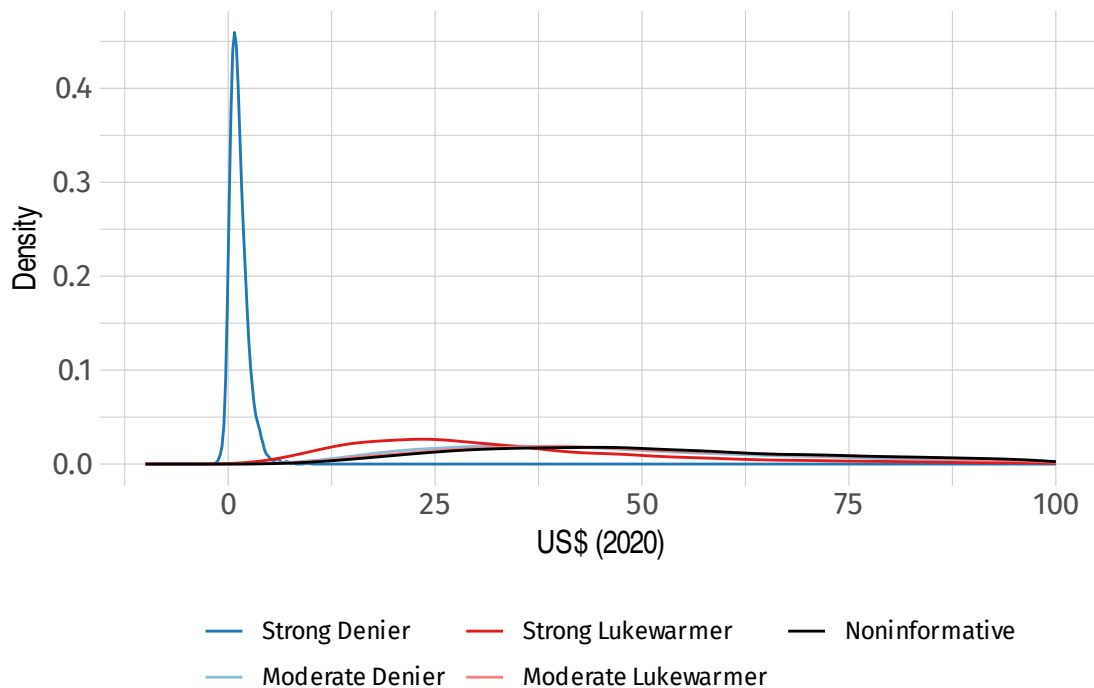
Welfare implications and the social cost of carbon

Figure SM9: Social cost of carbon (US$2020 per ton). SCC densities are generated by the MimiPAGE2009 model [Moore et al., 2018], with the regression posterior TCR distributions for each prior type serving as key inputs. Model defaults are used for all other parameters. The x-axis is truncated at 100 to aid visual inspection; the uppermost tails of the distributions being well in excess of the range given here.

References

Kevin Cowtan and Robert G. Way. Coverage bias in the HadCRUT4 temperature series and its impact on recent temperature trends. Quarterly Journal of the Royal Meteorological Society, 140(683):1935–1944, 2014. ISSN 1477-870X. doi: 10.1002/qj.2297. URL http://dx.doi.org/10.1002/qj.2297.

A. E. Dessler and P. M. Forster. An estimate of equilibrium climate sensitivity from interannual variability. Journal of Geophysical Research: Atmospheres, 123(16):8634–8645, 2018. doi: 10.1029/2018JD028481. URL https://agupubs.onlinelibrary.wiley.com/doi/abs/10.1029/2018JD028481.

William H. Greene. Econometric Analysis. Pearson Education, 6th edition, 2007.

Jeffrey B. Lewis and Drew A. Linzer. Estimating Regression Models in Which the Dependent Variable Is Based on Estimates. Political Analysis, 13(4):345–364, 2005. doi: 10.1093/pan/mpi026.

Kate Marvel, Gavin A. Schmidt, Ron L. Miller, and Larissa S. Nazarenko. Implications for climate sensitivity from the response to individual forcings. Nature Climate Change, 6(4):386–389, April 2016. doi: 10.1038/nclimate2888. URL http://dx.doi.org/10.1038/nclimate2888.

Frances C. Moore, James Rising, Niklas Lollo, Cecilia Springer, Valeri Vasquez, Alex Dolginow, Chris Hope, and David Anthoff. Mimi-PAGE, an open-source implementation of the PAGE09 integrated assessment model. Scientific Data, 5(1):1–8, 2018.

Colin P. Morice, John J. Kennedy, Nick A. Rayner, J.P. Winn, Emma Hogan, R.E. Killick, R.J.H. Dunn, T.J. Osborn, P.D. Jones, and I.R. Simpson. An Updated Assessment of Near-Surface Temperature Change From 1850: The HadCRUT5 Data Set. Journal of Geophysical Research: Atmospheres, page e2019JD032361, 2020. doi: 10.1029/2019JD032361. URL https://doi.org/10.1029/2019JD032361.

Drew T. Shindell. Inhomogeneous forcing and transient climate sensitivity. Nature Climate Change, 4:274–277, 9 March 2014. doi: 10.1038/nclimate2136. URL http://dx.doi.org/10.1038/nclimate2136.

Detlef P. Van Vuuren, Jae Edmonds, Mikiko Kainuma, Keywan Riahi, Allison Thomson, Kathy Hibbard, George C. Hurtt, Tom Kram, Volker Krey, Jean-Francois Lamarque, et al. The representative concentration pathways: an overview. Climatic Change, 109(1-2):5–31, 2011. doi: 10.1007/s10584-011-0148-z. URL http://dx.doi.org/10.1007/s10584-011-0148-z.